# The Influence of Monomer Chemistry on Radical Formation and Secondary Reactions During Electron-beam Polymerization

Nicole L. K. Thiher, Sage M. Schissel, and Julie L. P. Jessop

<sup>1</sup>University of Iowa, Chemical and Biochemical Engineering Department, Iowa City, IA

<sup>2</sup>PCT Ebeam and Integration, LLC, Davenport, IA

<sup>3</sup>Mississippi State University, School of Chemical Engineering, Mississippi State, MS

#### Abstract

The vast majority of industrial electron-beam (EB) polymerizations are initiated *via* radical mechanism. Because radicals drive EB polymerization, understanding their formation and secondary reactions can provide insight into polymerization kinetics and property development. Primary and initiating radicals were quantified by measuring  $G(R^*)$  and  $G(M^*)$ , respectively, for various acrylate and methacrylate monomers. Monomer chemistry was shown to impact primary radical formation; however, increased primary radical concentration did not necessarily correlate to increased conversion. Despite exhibiting high values of  $G(R^*)$ , methacrylates achieved very little conversion and had  $G(M^*)$  values near zero. Acrylates achieved much higher  $G(M^*)$  values and rates of polymerization compared to their methacrylate counterparts. Additionally, the efficiency of primary radicals converting to initiating radicals,  $f(M^*)$ , for each acrylate monomer was shown to be a good predictor of the amount of gel fraction formed during polymerization. Understanding radical formation and secondary radical reactions can help guide the structure/processing conditions/properties relationships that are currently underdeveloped for EB reactions.

# Keywords

Radiation chemical yield; G-value; (meth)acrylate; Raman spectroscopy

#### 1. Introduction

Since the 1980s, radical polymerization has been used to create nearly 45% of the synthetic polymers produced annually [1]. Hundreds of millions of metric tons of commodity polymers such as polypropylene, high-density polyethylene, low-density polyethylene, and polyvinyl chloride, as well as specialty polymers such as poly(ethylene terephthalate), other

polyesters, and polystyrene, are polymerized *via* radical polymerization each year [2]. These polymers are used in many diverse applications from construction materials and packaging to coatings and adhesives.

Energy input is generally required to initiate radical chain polymerization reactions [3]. The necessary energy can come in many forms, such as heat, light, or ionizing radiation [4]. Using ionizing radiation to initiate polymerization has advantages over more traditional initiation methods. For example, thermal initiation often requires a solvent to control heat input and the exotherm of polymerization [5]. In comparison, the typical formulations for ionizing-radiation-induced polymerizations are solvent free. Furthermore, initiators are not needed to start ionizing-radiation-induced polymerizations as is often the case in photo- or thermal polymerization [3], which eliminates the potential for initiator migration. The reduction in migration risk makes initiating polymerization with ionizing radiation especially appealing for food and medical packaging.

Gamma-rays, X-rays, and accelerated electrons are all examples of ionizing radiation that can be used to initiate polymerization. Both gamma-ray and X-ray equipment are used for industrial applications, but electron-beam (EB) accelerators dominate the ionizing-radiation-induced polymerization market. EB is used to create millions of metric tons of polymer products each year [6]. Still, relatively little is known about the kinetics of EB polymerization. The rapid reaction speeds and destructive nature of accelerated electrons preclude traditional reaction monitoring techniques from being used during real-time EB polymerizations and, thus, limit the ability to perform in-situ kinetic analysis.

EB polymerization reactions follow the three-step polymerization mechanism that was proposed by Flory in the 1930s and is universally accepted today (Scheme 1) [7,8]. The initiation step of radical polymerization requires energy input, and in the case of initiation with heat or light, an initiator molecule [9]. When energy is absorbed by these initiators (I), they decompose into predictable primary radical structures ( $R^{\bullet}$ ) [10,11]. In fact, the radical structures are so predictable that new initiators can be designed for specific applications.

	Thermal Polymerization	Photopolymerization (Non-ionizing Radiation)	Ionizing Radiation Polymerization	
Initiation	$I \xrightarrow{heat} 2R^{\bullet}$ $R^{\bullet} + M \to M^{\bullet}$	$I \xrightarrow{hv} 2R^{\bullet}$ $R^{\bullet} + M \to M^{\bullet}$	$A \xrightarrow{\bullet} R^{\bullet}$ $R^{\bullet} + M \rightarrow M^{\bullet}$	
Propagation	$M_n^{\bullet} + M \rightarrow M_{n+1}^{\bullet}$			
Termination	$M_n^{\bullet} + M_m^{\bullet} \to M_{n+m}$ and/or $M_n^{\bullet} + M_m^{\bullet} \to M_n + M_m$			

**Scheme 1.** The basic three-step polymerization mechanism for thermal-, photo-, and ionizing-radiation-initiated polymerization. While the initiation step differs, the propagation and termination steps are the same for all three polymerization types. I is an initiator,  $R^{\bullet}$  is a primary radial, M is a monomer,  $M^{\bullet}$  is an initiating radical,  $M_n^{\bullet}$  is a propagating radical, and A is any molecule in the formulation that can generate a primary radical when exposed to ionizing radiation. Scheme adapted from Ref. [3,12].

Contrastingly, initiation with ionizing radiation (including EB) requires no initiator molecule; rather, ionizing radiation can interact with virtually any molecule in the formulation (*A*), whether monomer, oligomer, and/or additive, and thus, initiation by ionizing radiation results in a multitude of different primary radical species [8]. Other researchers have used pulsed radiolysis and electron spin resonance (ESR) experiments to determine that one of the most common pathways to form this wide variety of primary radicals during EB exposure involves hydrogen abstraction [13]. While it is only in the formation of primary radicals that the mechanisms are expected to differ (Scheme 1), the non-selectivity of ionizing radiation can affect the polymerization reaction through the diversity and location of the primary radicals created.

Once primary radicals have formed, they have the ability to undergo secondary reactions (Scheme 2) [14]. This ability is true for all three mechanisms presented in Scheme 1. For instance, a primary radical can react with a monomer molecule (M) to form an initiating radical  $(M^{\bullet})$  that can go on to propagate a polymer chain (initiation). Note that the radical location must be on the C=C bond of the (meth)acrylate functional group for chain propagation to occur [3]; thus, all initiating radicals (as well as propagating radicals,  $M_n^{\bullet}$ ) have the same structure, regardless of the method of initiation or structure of the primary radical (Scheme 1). Other

possible secondary reactions shown in Scheme 2 include primary radicals reacting with one another to form a small molecule (recombination) or with a growing polymer chain to terminate polymerization (termination). Some primary radicals may be inert, and, as the polymer network develops, some primary radicals may become trapped and unable to react (inert/trapped). Additionally, ionizing radiation can cause primary radicals to form directly on the body of a growing polymer chains  $(P - R^*)$ , even in the absence of multifunctional monomers or oligomers or chain transfer. If these primary radicals react with a monomer molecule or an initiating radical, they can form a branch  $(B^* \text{ or } B)$ . They can also react with a branch or another primary radical on the body of polymer to form a crosslink (X) [12].

Recombination:  $R' + R' \rightarrow R_2$ Initiation:  $R' + M \rightarrow M'$ Branching:  $P - R' + M \rightarrow B'$  and/or  $P - R' + M_n' \rightarrow B$ Crosslinking:  $P - R' + B' \rightarrow X$  and/or  $P - R' + P - R' \rightarrow X$ Termination:  $M_n' + R' \rightarrow P_n$ Inert/Trapped:  $R' \rightarrow no\ reaction$ 

**Scheme 2.** Possible secondary reactions of primary radicals. Adapted from Ref. [14]. Note that  $P - R^*$  refers to a primary radical formed on the body of a polymer upon exposure to ionizing radiation; it does not refer to a propagating radical  $(M_n^*)$ . [12]

In thermal and photopolymerization, the predictability and uniformity (typically only one or two radical structures) of the primary radicals formed from initiators means that the occurrence of some of these secondary reactions can be influenced using initiator design.

Initiation can be given preference over recombination or termination using radical reactivity, for example, and is quantified by the initiator efficiency in thermal initiation and quantum yield in photoinitiation [3]. However, the diversity of primary radicals formed *via* ionizing radiation drastically increases the complexity and propensity of secondary reactions. That is, each possible primary radical structure (based on the formulation) may have a different predilection for a particular secondary reaction based on reactivity (*i.e.*, primary, secondary, and tertiary radical structure), steric hindrance, and the variety of other primary radicals in the vicinity. Parts of a formulation may be substituted to influence the quantity of primary radical formation but

also the properties of the polymer formed. Instead of a separate, controlled variable, as with thermal and photo-initiated systems, initiation is intrinsically entwined with the rest of the polymerization mechanism for ionizing radiation.

Because radicals are the driving force in the kinetics of EB polymerizations, quantifying radical formation and secondary radical reactions is critical to advancing the understanding of EB polymerizations. Previous work has been done to develop methods to quantify radicals created during EB exposure by calculating radiation chemical yields, also known as G-values [12,15]. In early literature, G-values were defined in terms of G(A), where "G(A) represents the number of events or chemical species of type A formed per 100 eV of energy absorbed" [16]. (The definition of the G-value has been updated to conform with SI units and is now reported in mol/J [17].) Using these methods, it is possible to calculate the total number of primary radicals that are formed via EB exposure (i.e., primary radical radiation chemical yield,  $G(R^{\bullet})$ ), as well as the number of radicals that go on to initiate polymerization (i.e., initiating radical radiation chemical yield,  $G(M^{\bullet})$ ). G-values of monomers have been calculated in the past [12, 15]; however, while monomer chemistry is wholly expected to be the driving factor behind G-values, a study to determine the impact of systematically altering monomer chemistry on the resulting Gvalues has not been undertaken. Since hydrogen abstraction has been shown to be a key factor in primary radical generation [13] and polymerization kinetics [18] in EB systems, the number of labile bonds a monomer contains was considered a reasonable focal point for such a systematic study. Previous research used a five-monomer series of acrylates to demonstrate the impact of abstractable hydrogens on EB-initiated polymerization kinetics [18], and this same series was chosen to expand this understanding to the relationship with radical formation and resulting polymer structure.

In addition, the monomer series was expanded to include methacrylate analogs of the acrylates. Comparing acrylates and methacrylates can provide a better understanding of the practical chemistry observed in industrial processes. The photopolymerization of acrylates and methacrylates is very common in industry [19-21]. In comparison, EB polymerization of acrylates is predominant in industry, and methacrylates are rarely used. The lack of methacrylates in EB polymerization may be the result of their slow reaction speeds. Studies have shown that the reaction rates of methacrylates are much slower than their analogous acrylate

counterparts [22,23]. Understanding how radical formation and secondary radical reactions differ between acrylates and methacrylates will help explain the differences in their polymerization kinetics.

In this paper, acrylate and methacrylate monomers with increasing number of abstractable hydrogens were investigated to determine the impact of monomer chemistry on radical formation and secondary radical reactions. A correlation was found between monomer chemical structure and primary radical radiation chemical yield,  $G(R^{\bullet})$ . Additionally, the initiating radical radiation chemical yield,  $G(M^{\bullet})$ , was shown to be impacted by the acrylate/methacrylate functionality. These data provide insight into why methacrylates notoriously suffer from low conversion during EB polymerizations. This research also provides a foundation for future investigations that can aid in the development of structure/processing conditions/properties relationships that are currently underdeveloped for EB polymerizations.

## 2. Experimental

#### 2.1. Materials

A series of five phenyl acrylate monomers, which have previously been used to investigate the impact of monomer chemistry on EB polymerization [18], was used in this study: phenyl acrylate (PA, TCI America); benzyl acrylate (BA, TCI America); 2-phenylethyl acrylate (PEA, Polysciences, Inc.); 2-phenoxyethyl acrylate (POEA, Millipore Sigma); 2-hydroxy-3-phenoxypropyl acrylate (HPOPA, TCI America) (Figure 1). This five-monomer series was selected because of the systematic increase in bonds between the acrylate and phenyl moieties across the series provides a controlled study of the impact of increasing number of labile bonds (primarily abstractable hydrogens). Additionally, the phenyl group is necessary for Raman spectroscopy measurements [24]. The series of acrylates was augmented with three analogous methacrylate monomers to investigate the impact of the methyl group on primary radical formation and secondary radical reactions: benzyl methacrylate (BMA, TCI America); 2-phenylethyl methacrylate (PEMA, Polysciences, Inc.); and 2-phenoxyethyl methacrylate (POEMA, TCI America).

The monomers were not washed of inhibitor because the impact of inhibitor was determined to be below the error of the measurements in this study. The photoinitiator 2,2-

dimethoxy-2-phenylacetophenone (DMPA, Sartomer) was used for photopolymerization studies. A free-radical inhibitor, 2,2-diphenyl-1-picrylhydrazyl (DPPH, Millipore Sigma), was used to quantify primary radicals, and a solvent, tetrahydrofuran (THF, Millipore Sigma), was used in the protocols that quantify initiating radicals and gel fraction. The THF was filtered and degassed before use. All other materials were used as received and stored at room temperature.

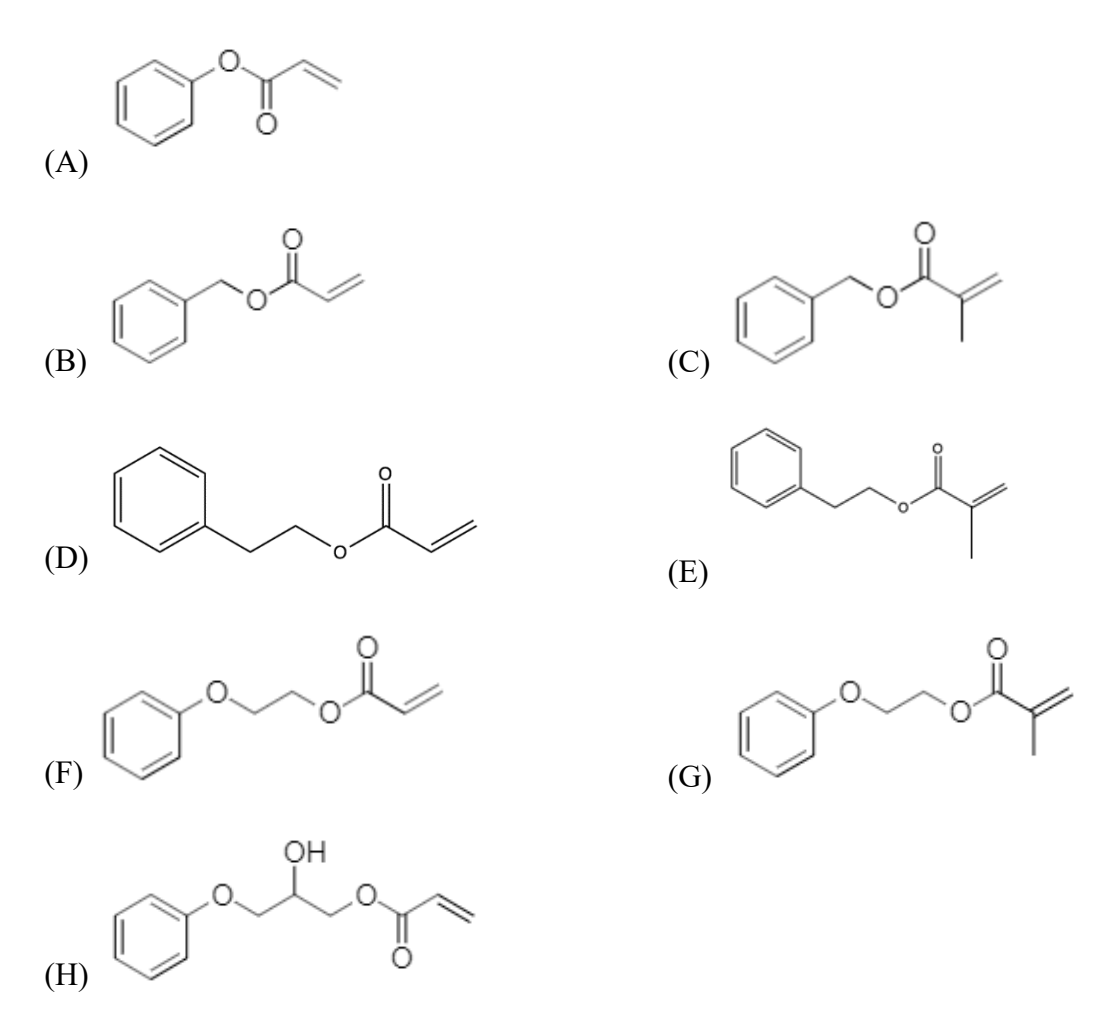


**Figure 1.** The chemical structures of the monomers used in this study: (A) PA, (B) BA, (C) BMA, (D) PEA, (E) PEMA, (F) POEA, (G) POEMA, and (H) HPOPA.

#### 2.2. Methods

## 2.2.1. Bond Dissociation Energy Calculations

Spartan Version 6.1 (Wavefunction, Inc.) was used to calculate the energy required to radicalize each monomer *via* hydrogen abstraction. A representative example of the hydrogen abstraction reactions considered for each monomer is provided in Scheme 3.

**Scheme 3.** Example of a hydrogen abstraction reaction for an acrylate monomer (PA) used to calculate the energy required to abstract a hydrogen in Spartan.

Although radicals can form through the cleavage of other bonds during exposure to ionizing radiation, the bond dissociation energy calculations are more complicated and would require significantly more processing time. Furthermore, pulse radiolysis studies of the radical structures created by EB exposure indicate that hydrogen abstraction is one of the most likely methods of radical formation [13]. The energy required to break a bond is dependent on the surrounding bonds; therefore, the energy required to abstract each hydrogen on a monomer ( $\Delta E$ ) was calculated independently using the following equation:

$$\Delta E = (E_{radicalized\ monomer} + E_{abstracted\ hvdrogen}) - E_{monomer}$$
 (1)

The *E*-values were determined using the  $\omega$ B97X-D/6-31G\* density functional model. An average value of hydrogen abstraction ( $\Delta E_{avg}$ ) was then calculated to represent each monomer's ability to generate primary radicals.

#### 2.2.2. Primary Radical Radiation Chemical Yield, $G(R^{\cdot})$

The methods used to determine primary radical radiation chemical yield have been described in detail previously [15], and only a brief outline of the method is presented here. (Note that the units of the *G*-value have been updated from radicals per 100 eV (used in early literature) to mol/J (the modern definition) by multiplying by 1.03 x  $10^{-7}$ .) To quantify primary radicals, an inhibitor was added to the formulation. When the inhibited formulation was exposed to the EB, primary radicals formed. These primary radicals then reacted with the inhibitor, inducing a color change. The disappearance of inhibitor is directly proportional to the rate of radical formation ( $R_R$ ) and was monitored using UV-Vis spectroscopy (DU-62)

Spectrophotometer, Beckman) (for example, see Figure 3 in Ref. [15]). After determining the rate of radical formation, Equation 1 was used to calculate  $G(R^{\bullet})$ , since the density  $(\rho)$  and dose rate  $\left(\frac{dD}{dt}\right)$  were known.

$$G(R') = \frac{R_R}{\rho \frac{dD}{dt}} \tag{2}$$

## 2.2.3. Initiating Radical Radiation Chemical Yield, G(M')

The methods used to determine initiating radical radiation chemical yield have been described in detail previously [15], and only a brief outline of the method is presented here. To quantify the initiating radicals, the rate of initiation  $(R_i)$  must first be determined. Assuming radical formation reaches steady state, Equation 2 can be used to determine the rate of EB initiation [3]. However, in order to calculate  $R_i$ , the monomer concentration ([M]), as well as the ratio of the kinetic constants of termination and propagation  $\left(\frac{k_t}{k_p^2}\right)$  and the rate of EB polymerization  $(R_p)$ , must first be determined.

$$R_i = \frac{k_t}{k_p^2} \frac{R_p^2}{[M]^2} \tag{3}$$

Existing methods to determine kinetic constants rely on real-time analysis, which is difficult to perform during EB polymerization because of the rapid reaction speeds and harsh nature of accelerated electrons. In addition to real-time analysis, determining the kinetic constants during photopolymerization requires changes in initiator concentrations, which is impossible to replicate in EB without changing reaction conditions because EB formulations contain no initiator. However, because the propagation and termination steps of UV and EB polymerization are the same (Scheme 1), the ratio of kinetic constants is assumed to be the same. Thus, the kinetic constants were determined through real-time Raman analysis (Mark II, Kaiser Optical Systems Inc.) of photopolymerization reactions and measurement of the number-averaged molecular weight using a gel permeation chromatography system (DAWN HELEOS-II, Wayatt Technology) (for example, see Figure 4 in Ref. [15]).

The rate of EB polymerization was determined by building a piecewise kinetic profile that related conversion to reaction time (Table 1 below). A graph of monomer concentration as a function of reaction time was created, and a best fit line, with slope equal to the rate of polymerization, was drawn through the linear portion of the graph (*i.e.*, excluding the inhibition period or conversion plateau if necessary). Monomer disappearance profiles created from Raman data were built by exposing different samples to increasing doses of ionizing radiation (for example, see Figure 5 in Ref. [15]). Other studies have shown that exposing multiple samples to different EB doses can result in different conversion values than exposing a single sample to the EB multiple times [14]. This previous study indicated that using multiple samples more closely mimics continuous EB, while using a single sample replicates pulsed-EB exposure. To build the piecewise profile, the dose and line speed of a lab-scale EB unit (EBLab, Comet Technologies, Inc.) were varied in combination to achieve a constant dose rate. The ratio of kinetic constants, rate of EB polymerization, and monomer concentration were then used to determine the rate of initiation. Finally, the initiating radical radiation yield  $(G(M^*))$  was calculated using Equation 4.

$$G(M^{\bullet}) = \frac{R_i}{\rho \frac{dD}{dt}} \tag{4}$$

#### 2.2.4. Conversion Measurements

Sample Preparation. Neat monomer was pipetted onto a glass slide, and a tape spacer was used to achieve a sample thickness of  $\sim \! 100~\mu m$ . EB polymerization took place on an EBLab unit (Comet Technologies, Inc.). The voltage was set at 200 kV to ensure uniform energy deposition through the entire depth of each sample. Nitrogen flow was used to reduce the oxygen concentration to less than 200 ppm to minimize the effect of oxygen inhibition. Ten exposure conditions were used for these experiments, all at a constant dose rate of  $197\pm 4~kGy/s$ . The dose and line speed combinations match those used to determine the radiation yield values and are shown in Table 1.

**Table 1.** Dose and line speed combinations used to create samples for conversion profiles.

Dose (kGy)	200	100	67	50	40	33	29	25	22	20
Line speed (m/min)	3	6	9	12	15	18	21	24	27	30

Raman microscopy. Raman microscopy was used to determine conversion of the samples after EB exposure. In order to eliminate error from instrumental variation and EB bombardment, a reference peak was used. Previous work has established the reaction peak at 1636 cm<sup>-1</sup> (indicative of the -C=C- bond in the acrylate moiety) and a reference peak at 1613 cm<sup>-1</sup> (indicative of the -C=C- bonds in the phenyl ring) [24]. Fractional conversion,  $\alpha$ , was calculated using the following equation:

$$\alpha = \left(1 - \frac{I_{rxn}(P)/I_{ref}(P)}{I_{rxn}(M)/I_{ref}(M)}\right) \tag{5}$$

where  $I_{rxn}(P)$  and  $I_{ref}(P)$  are the peak intensities of the reaction and reference peak of the polymer, respectively;  $I_{rxn}(M)$  and  $I_{ref}(M)$  are the peak intensities of the reaction and reference peak of the monomer [25].

EB-exposed samples were transferred to aluminum Q-panels for analysis. Raman spectra of the samples were collected using an optical microscope (DMLP Leica) connected to a modular research Raman spectrograph (HoloLab 5000R, Kaiser Optical Systems, Inc.) via a 100- $\mu$ m collection fiber. A single-mode excitation fiber carried an incident beam of 785-nm near-infrared laser to the sample through a 10x objective with a numerical aperture of 0.25 and a working distance of 5.8 mm. Laser power at the samples was ~8 mW. Spectra were collected with an exposure time of 30 seconds and 3 accumulations. Ten monomer spectra were collected and averaged to provide accurate values for  $I_{rxn}(M)$  and  $I_{ref}(M)$  to use in Equation 5. The error in the conversion measurements due to instrumental variation is expected to be  $\pm 0.05$ .

#### 2.2.5. Gel Fraction Measurements

Samples of monomer  $\sim \! 100~\mu m$  thick were created on a polyethylene terephthalate (PET) substrate using tape spacers. The samples were then exposed to the EB at a dose of 200 kGy with a line speed of 3 m/min. The accelerating voltage was set to 200 kV, and nitrogen flow was used to reduce the concentration of oxygen below 200 ppm.

After polymerization, the sample was removed from the PET backing and weighed before being placed in a vial. The vial was filled with THF and allowed to sit for 72 hours. The crosslinked polymer (gel) was separated from the soluble polymer using filter paper with a pore

size of 23 µm (Whatman). After filtration, the filter containing the gel was heated under vacuum for 3 hours to remove any excess solvent. Finally, the mass of the gel was recorded, and the gel fraction was calculated using the following equation:

$$Gel\ Fraction = \frac{Mass\ of\ Gel}{Mass\ of\ Polymer} \tag{6}$$

## 3. Results and Discussion

#### 3.1. Modeling Primary Radical Formation via Hydrogen Abstraction

Studies have shown that radical formation during EB polymerization may occur via hydrogen abstraction [13]. To model hydrogen abstraction, the average bond dissociation energies ( $\Delta E_{avg}$ ) of the acrylates and methacrylates were calculated using Spartan chemical modeling software (Figure 2). The energy of hydrogen abstraction was expected to correlate with the ability of each monomer to generate primary radicals upon EB exposure. Lower values of  $\Delta E_{avg}$  correspond to a lower energy requirement for a monomer to undergo hydrogen abstraction, and thus, a greater likelihood of forming primary radicals upon EB exposure.

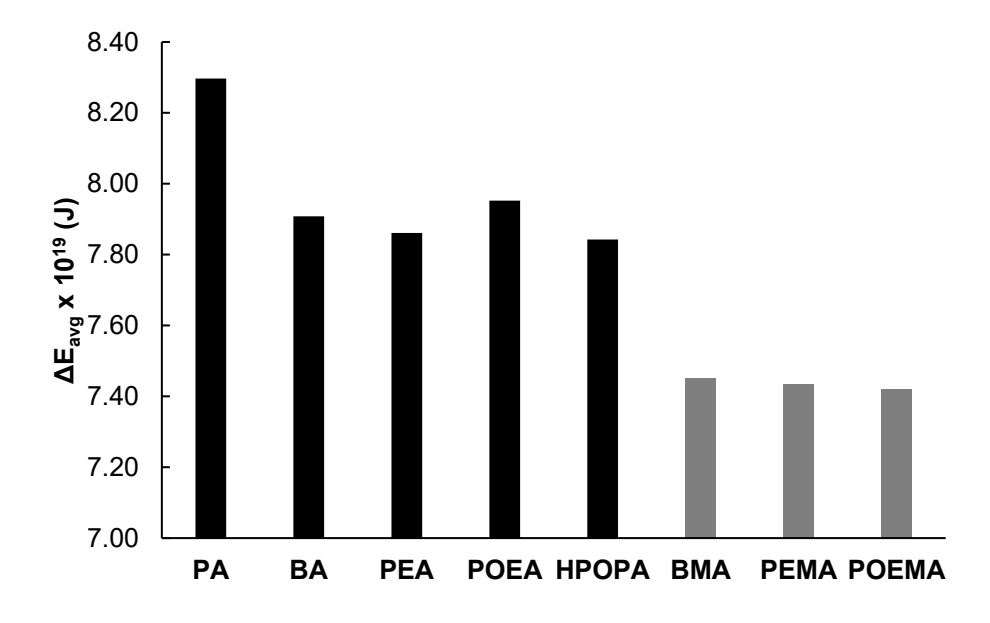


**Figure 2.** The average bond dissociation energy of the acrylate (black bars) and methacrylate (gray bars) monomers. In general, methacrylates are more likely to undergo hydrogen abstraction upon EB exposure because of their lower  $\Delta E_{avg}$  values.

The methacrylate monomers in this study have lower  $\Delta E_{avg}$  values than the acrylates. The methyl group on the methacrylates provides three additional low-energy C-H bonds compared to their otherwise identical acrylate counterparts. Because the C-H bond is relatively weak, additional C-H bonds increase the probability of a monomer undergoing hydrogen abstraction when bombarded with the EB.

In general, adding C-H bonds to the monomer between the phenyl and (meth)acrylate moieties decreases the  $\Delta E_{avg}$  values. For example, as the size of the acrylate monomers increases, the  $\Delta E_{avg}$  values decrease (i.e., monomers with a greater number of labile bonds have a greater probability of generating radicals when exposed to the EB). An exception to this trend occurs for the  $\Delta E_{avg}$  value of POEA. The monomer POEA is larger than PEA; however, the increase in size is due to the addition of an oxygen in the chain between the phenyl ring and acrylate moieties, not additional carbon-hydrogen bonds. Thus, PEA and POEA contain the same number of C-H bonds. The differences in their  $\Delta E_{avq}$  values indicate that not only are the number of abstractable hydrogens important, but their bond strength plays a role in determining their bond dissociation energies. One study to determine how monomer chemistry impacted EB crosslinking showed that monomers with many ester groups form less crosslinks upon EB exposure than similar monomers with fewer ester linkages [17]. Forming crosslinks, like conversion, is dependent on radical formation. Although this source investigated the effects of EB exposure on polymers rather than polymerization, radical formation is likely chemistry dependent in both cases. This structural difference may help explain why, despite being smaller molecules, BA and PEA have a lower  $\Delta E_{avg}$  values than POEA. This anomaly is not apparent when comparing the  $\Delta E_{avg}$  values of the methacrylates. The addition of the methyl group must reduce the impact of the added oxygen in the structure of POEMA.

#### 3.2. Primary Radical Reactions

Primary radical formation was quantified by calculating  $G(R^{\bullet})$  for each monomer using the inhibitor method described in Section 2.2.2. Methacrylates exhibited higher values of  $G(R^{\bullet})$  compared to their acrylate counterparts (Figure 3). The higher radical concentration of the methacrylates compared to the acrylates was expected because of their low  $\Delta E_{avg}$  values. The  $\Delta E_{avg}$  values of the methacrylates indicate that, as monomer size and number of labile bonds

increase, radical formation becomes easier. This prediction is confirmed when comparing the  $G(R^{\bullet})$  values of the methacrylates.

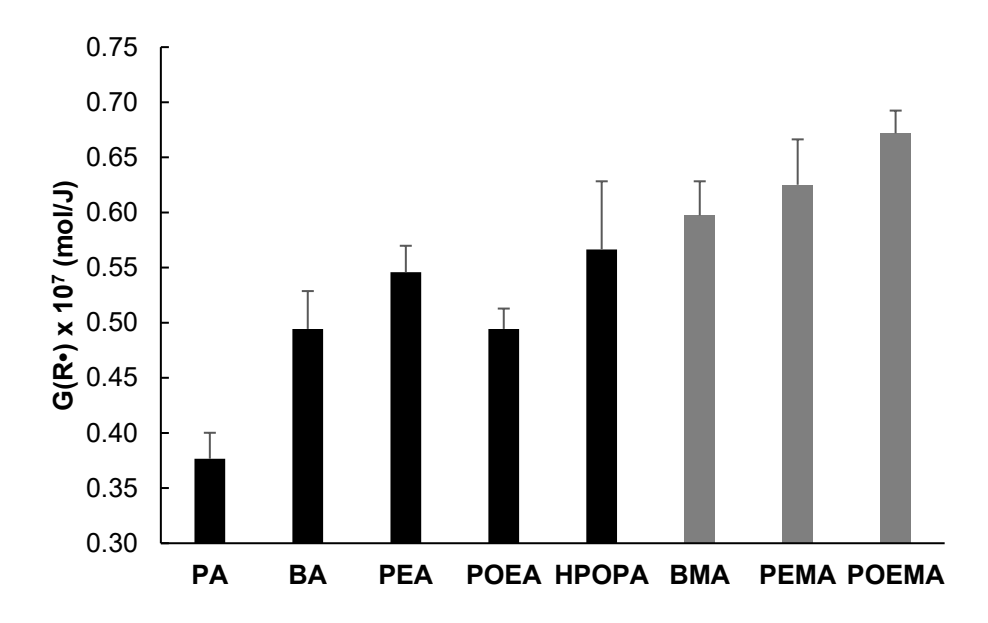


**Figure 3.** Primary radical formation quantified by measuring  $G(R^*)$  for each monomer. Methacrylates (gray bars) form more primary radicals upon EB exposure compared to their acrylate counterparts (black bars).

In general, the  $G(R^{\bullet})$  values of the acrylates also increased with increasing monomer size. As predicted by the  $\Delta E_{avg}$  calculations, POEA is an exception to this trend. For POEA, the addition of the oxygen between the acrylate and phenyl moieties increases the stability of the surrounding C-H bonds and suppresses radical formation.

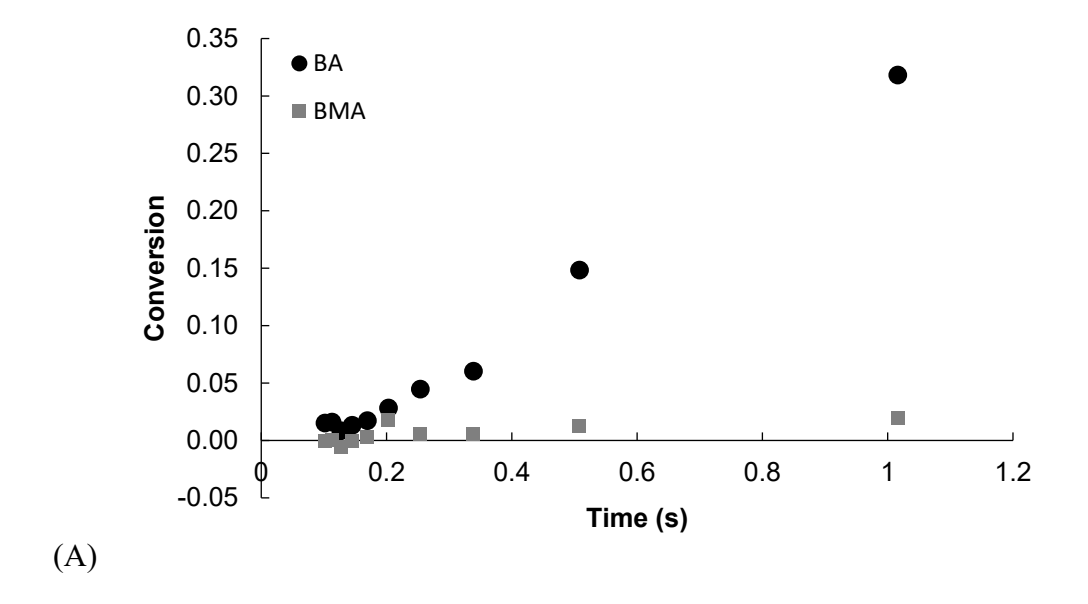
These results indicate that theoretical calculations of  $\Delta E_{avg}$  are strongly correlated to experimental  $G(R^{\bullet})$  values. Modeling  $\Delta E_{avg}$  of a monomer is relatively easy and requires only a software package. Contrastingly, experiments to determine  $G(R^{\bullet})$  of a monomer requires materials, equipment, and significantly more time. Thus, it may be advantageous to predict a monomer's ability to generate primary radicals using calculations of  $\Delta E_{avg}$  before any experiments take place.

## 3.3. Conversion and $R_p$ of Acrylates vs. Methacrylates

Raman microscopy was used to measure conversion of the acrylate monomers and their methacrylate analogs after EB exposure to investigate the impact of primary radical

concentration on conversion (Figure 4). Overall, there was not a strong correlation between primary radical concentration and conversion for either the acrylates or the methacrylates.

The acrylate conversion profiles, as anticipated, increased with increasing dose and time. The fractional conversion of BA reached nearly 0.35 at a dose of 200 kGy (t = 1 s), while PEA and POEA both achieved final conversions near 0.2. However, neither the final conversion values nor the speed of reaction seem to be related to the primary radical concentrations quantified by calculating  $G(R^{\bullet})$ . Based on the  $G(R^{\bullet})$  values, PEA generates the most primary radicals followed by BA and then POEA. Yet, BA reacts the quickest and achieves the highest final conversion, and the final conversions of PEA and POEA are nearly identical. The lack of relationships between  $G(R^{\bullet})$  and ultimate conversion or speed of reaction underscores that the secondary radical reactions, described in Scheme 2, have a noticeable impact on polymerization kinetics.



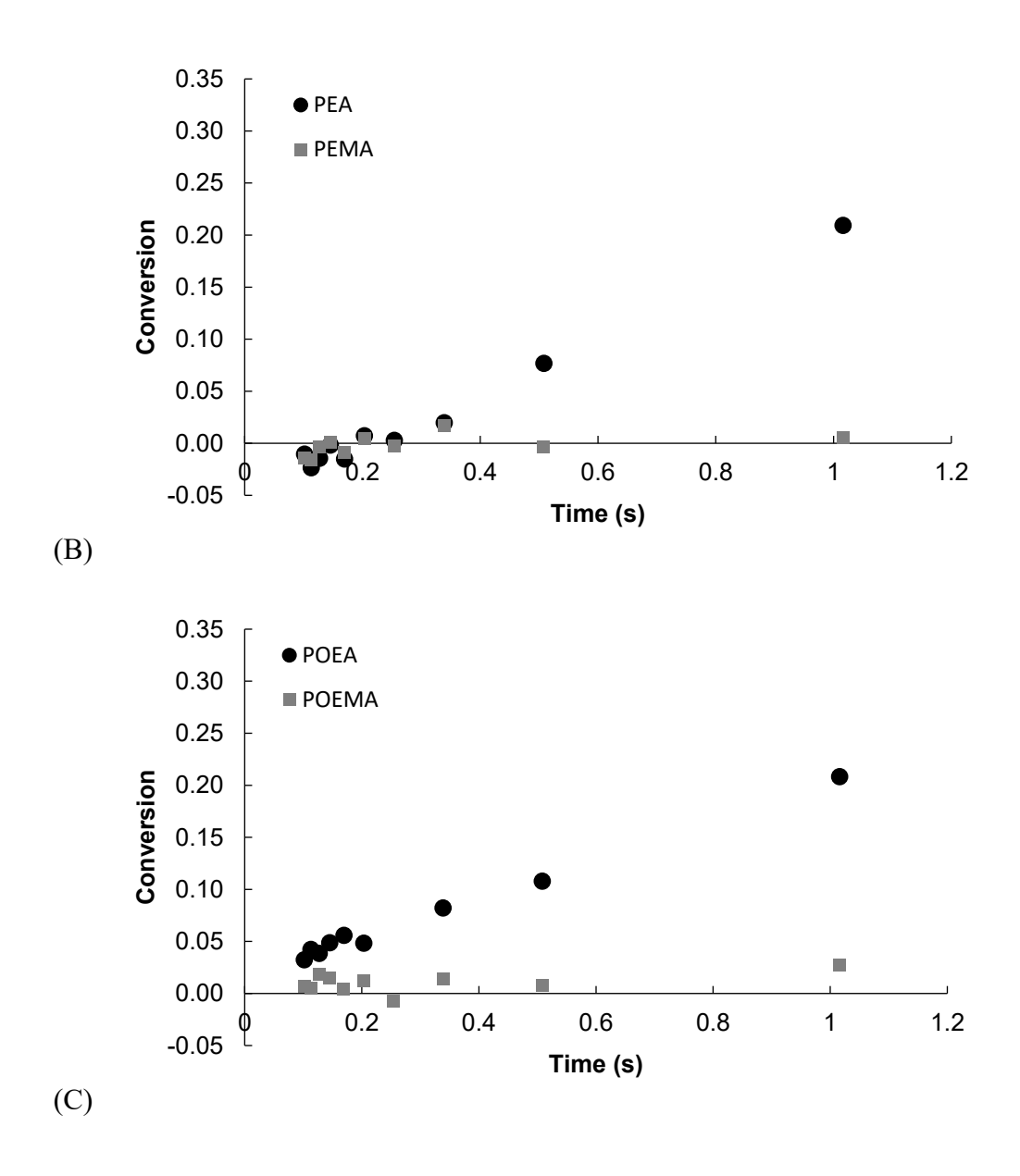


**Figure 4.** Piecewise conversion profiles of the acrylate monomers and their methacrylate analogs: (A) BA vs. BMA, (B) PEA vs. PEMA, and (C) POEA and POEMA. Acrylates are able to achieve significant conversion upon EB exposure, while the conversion of the methacrylates are near zero regardless of the dose delivered.

The methacrylates provide even more evidence that primary radical concentration is not a good predictor of final conversion. All of the methacrylates had higher  $G(R^*)$  values than their acrylate counterparts, thus generating more primary radicals; however, the methacrylates achieved no appreciable conversion, even when exposed to the highest dose at 200 kGy. In fact, the highest fractional conversion achieved by any of the methacrylates in this study was 0.03.

The low final conversion of the methacrylates compared to the acrylates is not necessarily surprising. Other researchers have observed slow reaction rates of methacrylates compared to acrylates during photopolymerization reactions [26-30]. The slow  $R_p$  values of methacrylates have been attributed to the stability of the tertiary propagating methacrylate radical (in comparison to the secondary propagating acrylate radical), as well as the increased steric hindrance caused by the additional C-H bonds [31,32]. One study reported a 7-fold decrease in the rate of polymerization of methacrylates compared to their identical acrylate counterparts during photopolymerization [23].

Using the conversion data, the rate of polymerization  $(R_p)$  was calculated for the acrylate and methacrylate pairs in this study (Table 2). Because the methacrylates achieved very little conversion, their rates of polymerization are all around zero; whereas, the  $R_p$  values for the acrylates are all higher than 1 mol/L·s. Thus, the difference in  $R_p$  of the EB-initiated acrylates and methacrylates chosen for this study is even more pronounced than what was reported in the photopolymerization literature. The methacrylates in this study experienced  $R_p$  values 15 to 18 times lower than their acrylate counterparts.

**Table 2.**  $G(R^{\bullet})$ ,  $R_p$ , and conversion after 1 s of EB exposure for the monomer pairs used in this study. Increased concentration of primary radicals does not necessarily result in more or faster polymer conversion.

Monomer	<i>G(R')</i> (mol/J)	$R_p \text{ (mol/L} \cdot s)$	1 s Conversion
BA	0.49	2.25	0.32
PEA	0.55	1.46	0.21
POEA	0.49	1.34	0.21
	1		
BMA	0.60	0.12	0.02
PEMA	0.63	0.08	0.01
POEMA	0.67	0.09	0.03

The greater reduction in  $R_p$  of methacrylates during EB initiation compared to UV initiation could simply be the result of the difference in typical reaction times for the two initiation mechanisms. Industrial EB polymerizations (and those reported in this study) take place in a few seconds or even fractions of seconds, while photopolymerization can take tens of seconds [23, 33]. The short reaction time of EB polymerizations means the stable initiating

methyl radicals, with increased steric hindrance, have less time to react and induce conversion compared to relatively long UV exposures.

In addition, it is also possible that the stability of the primary radical structures contribute to the slow rate of EB-initiated methacrylate polymerization. As previously discussed (Section 1), primary radicals are formed in UV-initiated systems through the decomposition of photoinitiator, resulting in predictable primary radical structures specifically designed to induce polymerization (Scheme 1) [3]. Contrastingly, primary radicals during EB initiation are formed directly on virtually any molecule in the system, resulting in numerous potential primary radical structures [8]. The lack of conversion of the EB-initiated methacrylates may result from the formation of more stable primary radicals compared to those that form *via* UV initiation. Without knowing the structures of the primary radicals formed *via* EB initiation, it is difficult to predict how likely it is for a primary radical to undergo the secondary reaction necessary to become an initiating radical.

## 3.4. Secondary Radical Reactions

Although methacrylates formed more primary radicals than their acrylate counterparts, conversion values from Section 3.3 show that primary radical formation is not the major factor in determining if conversion will occur when a monomer is exposed to the EB. When primary radicals are formed during EB exposure, they can undergo numerous secondary reactions (Scheme 2). Conversion of monomer to polymer will only take place if primary radicals react to form initiating radicals. Thus, the initiating radical radiation chemical yield  $G(M^{\bullet})$  is likely a better indicator of whether a monomer will achieve conversion upon EB exposure. The  $G(M^{\bullet})$  values of the acrylates were calculated using Equations 3 and 4 (Table 3). Because  $G(M^{\bullet})$  is dependent on  $R_p$  and none of the methacrylates achieved  $R_p$  values much above zero, the  $G(M^{\bullet})$  values of the all the methacrylates in this study were estimated to be  $\sim$ 0.

**Table 3.**  $G(R^{\bullet})$ ,  $G(M^{\bullet})$ , and  $f(M^{\bullet})$  values of EB-polymerized acrylate monomers.

Monomer	$G(R^{\bullet})$	$G(M^{\bullet})$	f(M')
BA	0.48	0.33	0.69
PEA	0.53	0.18	0.34
POEA	0.48	0.10	0.21

Before comparing  $G(R^{\bullet})$  and  $G(M^{\bullet})$  values, it is important to note that the calculation of  $G(M^{\bullet})$  relies on the assumption that the ratio of kinetic constants of propagation and termination is the same for EB and UV initiation. This assumption has been made by researchers in the past [34-36], but no studies have been found that confirm its validity. Therefore, the implications of this assumption must be considered when directly comparing  $G(R^{\bullet})$  and  $G(M^{\bullet})$  values. Here, all  $G(R^{\bullet}) > G(M^{\bullet})$ , which is expected since not all primary radicals will yield initiating radicals. Furthermore, these G-values are similar to G-values reported in previous literature [12], which gives confidence that the assumption is reasonable for this situation.

For the acrylates, high values of  $G(M^{\bullet})$  correspond to increased polymerization rates (Table 2). Based on the classic kinetic equation,  $R_p$  has a first-order dependence on initiating radical concentration [3]; thus, the increase in rate with increasing initiating radical concentration is expected. Increasing  $G(M^{\bullet})$  increases  $R_p$ , but that does not necessarily translate to an increase in final conversion (Tables 2 and 3). BA has the highest  $G(M^{\bullet})$  value and achieves the greatest final conversion. The final conversions of PEA and POEA are both lower than that of BA. However, the PEA and POEA conversions are nearly identical, despite PEA having a  $G(M^{\bullet})$  that is nearly double that of POEA. The difference in  $G(M^{\bullet})$  of PEA and POEA indicates that, while  $G(M^{\bullet})$  is more strongly correlated to conversion than  $G(R^{\bullet})$ , initiating radicals are not the only factor that influences conversion.

To better understand the secondary radical reactions, the ratio of primary radicals that react to form initiating radicals  $(f(M^{\bullet}))$  can be calculated using the following equation:

$$f(M^{\bullet}) = \frac{G(M^{\bullet})}{G(R^{\bullet})} \tag{7}$$

High values of  $f(M^{\bullet})$  indicate that most of the primary radicals go on to initiate polymerization. Monomers with lower values of  $f(M^{\bullet})$  must undergo other secondary reactions, which can have an impact on network formation and ultimate conversion.

The f(M') values of the acrylates were calculated using Equation 7 (Table 3). Because the f(M') values of the methacrylates would be  $\sim 0$  due to  $\sim 0$  values of G(M'), the methacrylate monomers are not considered in this discussion. These results indicate that, as the number of

labile bonds on a monomer increases,  $f(M^*)$  decreases. The decrease in  $f(M^*)$  suggests that monomers with more labile bonds, which may be better at producing primary radicals, are less efficient at undergoing the secondary reaction necessary to produce initiating radicals. The additional reactive sites on larger monomers provide more locations for other secondary reactions, such as crosslinking or chain transfer, to take place compared smaller monomers. Thus, many of the primary radicals that form on monomers with more labile bonds may undergo secondary reactions other than initiation, suppressing the value of  $G(M^*)$ . For example, POEA is a larger monomer with a lower value of  $f(M^*)$  compared to PEA. The difference in  $f(M^*)$  of PEA and POEA could help explain why these monomers achieve similar final conversions despite POEA having a higher  $G(M^*)$ . For POEA, only 21% of the primary radicals go on to initiate polymerization, leaving 79% of the radicals to undergo other reactions described in Scheme 2; comparatively, 34% of PEA's primary radicals become initiating radicals. Having a large number of radicals participate in reactions other than initiation may cause changes in the polymer network [37].

Most of the secondary radical reactions are difficult to quantify; however, the amount of crosslinked vs. linear polymer can easily be determined by measuring gel fraction. The gel fraction of the acrylate polymers created from 1 s EB exposure was determined to investigate the extent to which radicals participate in the crosslinking secondary reaction. Monomers with low values of  $f(M^*)$  produced more gel and, thus, had more highly crosslinked networks (Figure 5). The gel fraction of BA, which had the highest  $f(M^*)$  value, was nearly zero, meaning that the sample was almost entirely made up of linear (or branched) polymer chains. POEA had the lowest  $f(M^*)$  value and achieved a final fractional conversion of  $0.21\pm0.05$  and a gel fraction of  $0.25\pm0.04$ , which indicates that all of the POEA polymer that formed was crosslinked. PEA fell somewhere in between, reaching a fractional conversion of  $0.21\pm0.05$  and a gel fraction of  $0.14\pm0.05$ . The gel fraction of PEA is less than the fractional conversion, indicating that the polymer is made up of both linear and crosslinked polymer chains.

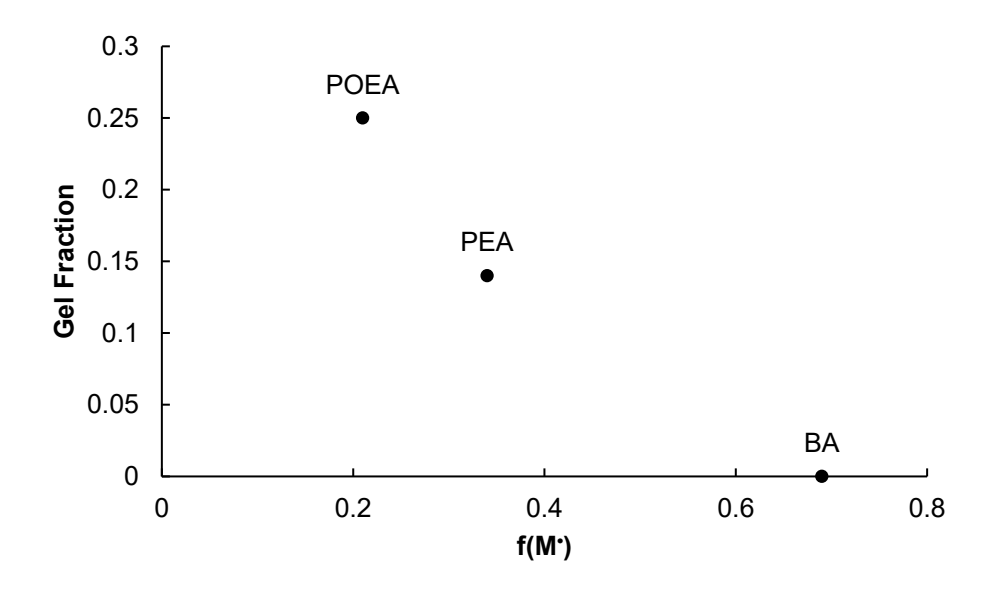


**Figure 5.** For the acrylate monomers, an increase in gel fraction is observed as the ratio of initiating radicals to primary radicals  $(f(M^{\bullet}))$  decreases.

Figure 5 shows that the  $f(M^{\bullet})$  value of a monomer is a good indicator of the amount of crosslinking in the resulting polymer network. However, predicting crosslinking does not give a complete picture of the final properties of a polymer. Values of  $G(R^{\bullet})$ ,  $G(M^{\bullet})$ , or  $f(M^{\bullet})$  alone do not have a strong correlation to final conversion. Thus, it is necessary to consider not only the primary and initiating radicals, but the other secondary radical reactions described in Scheme 2. For example, increasing the amount of termination caused by primary radicals could lead to small chain lengths and even suppress final conversion. Both changes in chain length and conversion could have a significant impact on final polymer properties. Based on the results of this research, it is clear that determining the factors that influence what secondary reaction a primary radical will undergo is key to understanding EB kinetics and predicting final polymer properties.

## 4. Conclusions

Radical formation and secondary radical reactions initiated via EB exposure are dependent on monomer chemistry. Chemical modeling software can be used to predict the ability of a monomer to form primary radicals during EB polymerization by calculating  $\Delta E_{avg}$ . There was a strong correlation between  $\Delta E_{avg}$  and  $G(R^{\bullet})$ . However, high concentrations of primary radicals did not necessarily translate into increased conversion. The methacrylates in this study

had higher values of  $G(R^{\bullet})$  than their acrylate counterparts, but the methacrylates failed to achieve any appreciable conversion during EB exposure.

Secondary radical reactions were shown to have an impact on conversion for the acrylate monomers. The  $G(M^{\bullet})$  value of each monomer was calculated to quantify the initiating radicals formed during EB exposure. A correlation between the rate of polymerization and  $G(M^{\bullet})$ , which followed classical kinetics, was observed for the acrylates in this study. Other secondary radical reactions, such as crosslinking, were shown to have an impact on network formation and final conversion.

Ultimately, understanding radical formation and secondary radical reactions is critical to developing structure/processing conditions/properties relationships for EB polymerization.

Indeed, the results of this study highlight the intricacy of the kinetics of EB polymerization. The relationships among radical formation, secondary radical reactions, and polymer conversion are complex and dependent on monomer chemistry. Future work should focus on determining the structures of the primary radicals formed using EB initiation; such an endeavor will require computer modeling possibly paired with pulsed radiolysis and/or ESR experiments. In addition, it is important to expand the radical relationships beyond one-component formulations of acrylates and methacrylates into mixtures of monomers and oligomers, which are widely used in industry, in order to guide EB formulation development. Finally, this study focused on EB initiation, but the relationships between monomer chemistry and radical formation, as well as secondary radical reactions, may be applicable to polymerization with other initiating sources. Further investigation into other initiation sources, especially other types of ionizing radiation, will aid in the development of general relationships between chemistry and radial formation that can be used to predict and control polymer properties.

## 5. Acknowledgements

This work was supported by the National Science Foundation [grant number 1804641].

## 6. References

- 1. Braun, D., Origins and Development of Initiation of Free Radical Polymerization Processes. *International Journal of Polymer Science*, 2009. **2009**.
- 2. Nesvadba, P., Radical Polymerization in Industry, in *Encyclopedia of Radicals in Chemistry, Biology and Materials*. 2012: John Wiley & Sons, Ltd.

- 3. Odian, G., *Principles of Polymerization*. 4th ed. 2004, Hoboken, NJ: John Wiley & Sons, Inc.
- 4. Fouassier, J.P., On the structure/properties relationships in photoinitiators of polymerization. *Polymer Engineering & Science*, 1995. **35**(12): p. 1061-1065.
- 5. Moad, G. and D.H. Solomon, *The chemistry of radical polymerization*. 2006, New York, NY: Elsevier.
- 6. Cohen, G., UV/EB Market Trends. *RadTech Report*, 2012. **26**(2): p. 44-48.
- 7. Flory, P.J., The Mechanism of Vinyl Polymerizations 1. *J. Am. Chem. Soc.*, 1937. **59**(2): p. 241-253.
- 8. Chapiro, A., *Radiation chemistry of polymeric systems*. 1962, New York, NY: Interscience Publishers.
- 9. Massy, J., *A Little Book about BIG Chemistry: The Story of Man-Made Polymers*. 2017: Springer International Publishing.
- 10. Ravve, A., Photosensitizers and Photoinitiators. 2006, New York, NY: Springer. 23-122.
- 11. Fouassier, J.-P., *Photoinitiation, Photopolymerization, and Photocuring: Fundamentals and Applications.* 1995, New York, NY: Hanser.
- 12. Thiher, N.L.K., S.M. Schissel, and J.L.P. Jessop, Analysis of methods to determine G-values of monomers polymerized via ionizing radiation. *Radiation Physics and Chemistry*, 2019. **165**: p. 108394.
- 13. Knolle, W. and R. Mehnert, On the mechanism of the electron-initiated curing of acrylates. *Radiation Physics and Chemistry*, 1995. **46**(4-6): p. 963-974.
- 14. Richter, K.B., *Pulsed electron beam curing of polymer coatings*. Ph.D. Thesis, University of Michigan, Ann Arbor, MI, 2007.
- 15. Thiher, N.L.K., S.M. Schissel, and J.L.P. Jessop, Counting Radical: Methods to Measure Radiation Yields of Monomers in EB Polymerization. *UV+EB Technology*, 2019. **5**(2): p. 32-40.
- 16. McNair, A., ICRU Report 33 Radiation Quantities and Units Pub: International Commission on Radiation Units and Measurements, Washington D.C. USA issued 15 April 1980, pp.25. *Journal of Labelled Compounds and Radiopharmaceuticals*, 1981. **18**(9): p. 1398-1398.
- 17. Makuuchi, K. and S. Cheng, *Radiation processing of polymer materials and its industrial applications*. 2011, Hoboken, NJ: John Wiley & Sons, Inc.
- 18. Schissel, S.M., S.C. Lapin, and J.L.P. Jessop, Characterization and prediction of monomer-based dose rate effects in electron-beam polymerization. *Radiation Physics and Chemistry*, 2017. **141**: p. 41-49.
- 19. Fink, J.K., Acrylic Dental Fillers Chapter 19 in *Reactive Polymers: Fundamentals and Applications*, 2nd ed. 2013: Elsevier, Inc. p. 453-474.
- 20. Crivello, J.V., Photopolymerization in *Polymer Science: A Comprehensive Reference*, 1st ed. 2012: Elsevier Science. p. 919-955.

- 21. Andrzejewska, E., Chapter 2 Free Radical Photopolymerization of Multifunctional Monomers in *Three-Dimensional Microfabrication Using Two-photon Polymerization*. 2016: William Andrew Publishing, p. 62-81.
- 22. Peppas, N.A., Kinetics of the crystallization of crosslinked poly(vinyl alcohol) films by slow evaporation of hydrogels in *Chemistry and properties of crosslinked polymers*, edited by S. S. Labana. 1977, New York, NY: Academic Press. p. 469-479.
- 23. Kurdikar, D.L. and N.A. Peppas, A kinetic study of diacrylate photopolymerizations. *Polymer*, 1994. **35**(5): p. 1004-1011.
- 24. Schissel, S.M., S.C. Lapin, and J.L.P. Jessop, Internal Reference Validation for EB-Cured Polymer Conversions Measured via Raman Spectroscopy. *RadTech Report*, 2014. **28**(4): p. 46-50.
- 25. Cai, Y. and J.L.P. Jessop, Decreased oxygen inhibition in photopolymerized acrylate/epoxide hybrid polymer coatings as demonstrated by Raman spectroscopy. *Polymer*, 2006. **47**(19): p. 6560-6566.
- 26. Anseth, K.S., C.M. Wang, and C.N. Bowman, Reaction behaviour and kinetic constants for photopolymerizations of multi(meth)acrylate monomers. *Polymer*, 1994. **35**(15): p. 3243-3250.
- 27. Scherzer, T., VUV-Induced Photopolymerization of Acrylates. *Macromolecular Chemistry and Physics*, 2012. **213**(3): p. 324-334.
- 28. Ghorpade, R., et al., Photopolymerization kinetics of 2-phenylethyl (meth)acrylates studied by photo DSC. *J. Polym. Res.*, 2012. **19**(2): p. 1-8.
- 29. Takács, E. and L. Wojnárovits, Comparison of the reactivity of acrylate and methacrylate monomers. *Radiation Physics and Chemistry*, 1995. **46**(4, Part 2): p. 1007-1010.
- 30. McCurdy, K.G. and K.J. Laidler, Rates of polymerization of acrylates and methacrylates in emulsion systems. *Canadian Journal of Chemistry*, 1964. **42**(4): p. 825-829.
- 31. Doetschman, D.C., R.C. Mehlenbacher, and D. Cywar, Stable free radicals produced in acrylate and methacrylate free radical polymerization: Comparative EPR studies of structure and the effects of cross-linking. *Macromolecules*, 1996. **29**(5): p. 1807-1816.
- 32. Matyjaszewski, K. and T.P. Davis, *Handbook of radical polymerization*. 2002: Hoboken, NJ: Wiley-Interscience.
- 33. Schissel, S.M. and J.L.P. Jessop, Quantitative Comparison of Photo- and Electron-beam Polymerizations Based on Equivalent Initiation Energy. *Radiation Physics and Chemistry*, 2019. **157**: p. 72-83.
- 34. Matheson, M.S., et al., Rate Constants in Free Radical Polymerization. III. Styrene 1. *J. Am. Chem. Soc.*, 1951. **73**(4): p. 1700-1706.
- 35. Tobolsky, A.V. and B. Baysal, A review of rates of initiation in vinyl polymerization: Styrene and methyl methacrylate. *J. Polym. Sci.*, 1953. **11**(5): p. 471-486.
- 36. Tobolsky, A.V. and J. Offenbach, Kinetic constants for styrene polymerization. *J. Polym. Sci.*, 1955. **16**(82): p. 311-314.
- 37. Wartewig, S. and G. Helmis, *Physics of Polymer Networks*. 1992, Darmstadt: Steinkopff.